Supporting Information

Liquid-like Nanofluids Mediated Modification of Solar-assisted Sponge for Highly Efficient Cleanup and Recycling of a Viscous Crude Oil Spill

*Yushan Li,[‡a] Song Yan,[‡a] Ziwei Li,[‡c] Siwei Xiong,[a] Shiwen Yang,[*a] Luoxin Wang,[a] Hua Wang,[a] Xianjie Wen,[*b] Pingan Song,[d] Xianze Yin [*a]*

[a] College of Materials Science and Engineering, State Key Laboratory of New Textile Materials & Advanced Processing Technology, Wuhan Textile University, Wuhan 430073, China.

[b] Department of Anesthesiology, The Second People's Hospital of Foshan city, Foshan 528000, Guangdong Province, China.

[c] College of Materials Science and Engineering, Guilin University of Technology, Guilin 541004, China.

[d] Centre for Future Materials, University of Southern Queensland, Springfield, QLD 4300, Australia

* Corresponding Author

* E-mail: swyang@wtu.edu.cn

* E-mail: xjwen166@163.com

* E-mail: yinxianze@wtu.edu.cn

‡ These authors contributed equally to this work.

Section S1: The preparation of SiO$_2$ nanofluids (SiO$_2$ nfs)

1.0 g SiO$_2$ powder were dispersed in 50 mL of deionized water and ultrasonicated for 30 min. Then 10 mL of DC5700 in methanol (40 mass %) were dropwise added and aged for 24 h at room temperature by gently shaking it periodically. Next, the solution was separated by extraction filtration and washed three times in turn with water and methanol. The separated light yellow precipitate was dried at 65 °C for 24 h in a vacuum oven to obtain the SiO$_2$ chlorine salt. Subsequently, the SiO$_2$ chlorine salt was added in 15 mass % solution of NPEP in water/chloroform (volume ratio = 2:3) while stirring at 50 °C for 24 h. Finally, the resultant solution was dried and extracted three times in turn. The solid was also dispersed in chloroform, centrifuged, and then dried in a vacuum oven at 65 °C for 48 h to obtain yellow nanofluids at room temperature..
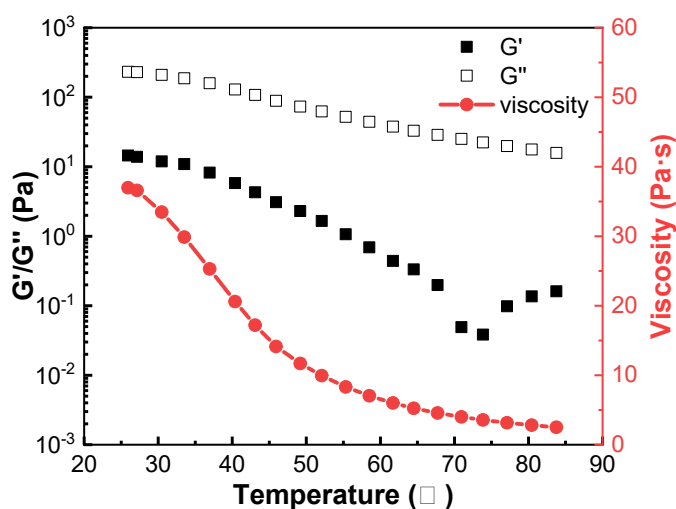
Section S2: Supporting figures

Figure S1. Rheological behavior of SiO$_2$ nfs. All the above tests were conducted at an environmental temperature of 25 °C.
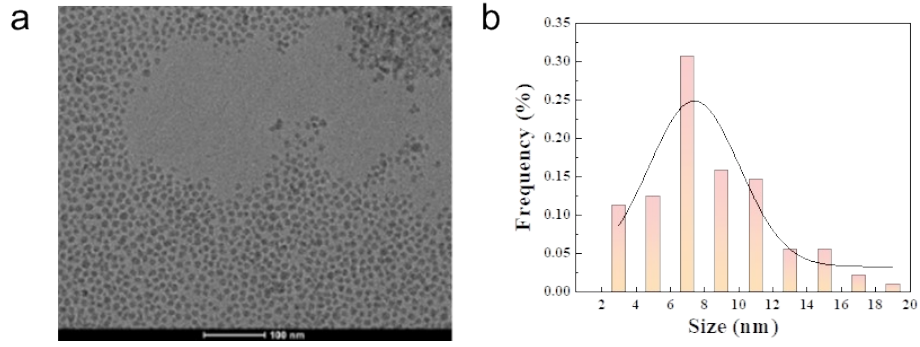
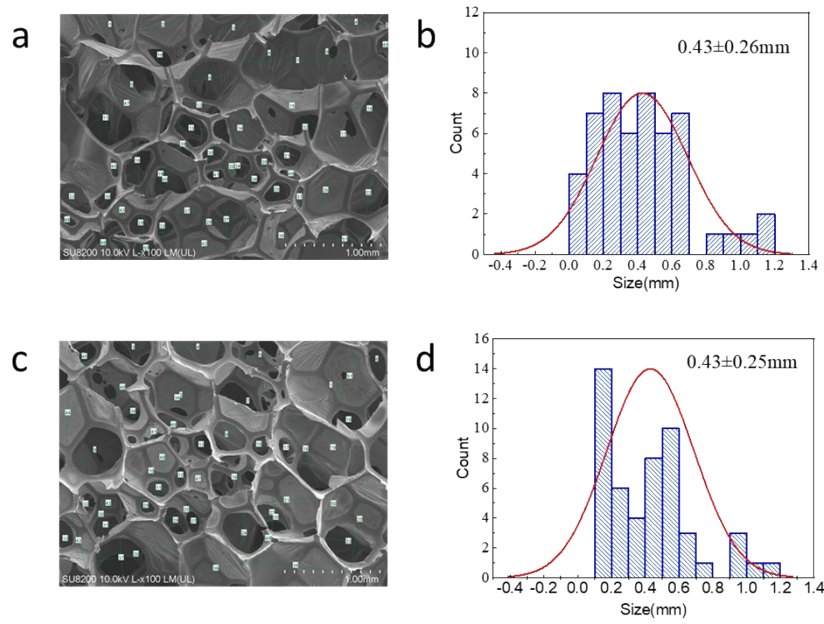**Figure S2.** (a) TEM images of SiO_2 nfs. (b) Size distribution of SiO_2 nfs.

Figure S3. SEM images of the (a) PUS sponges and (c) PSiNFs@PU, Statistical data of pore

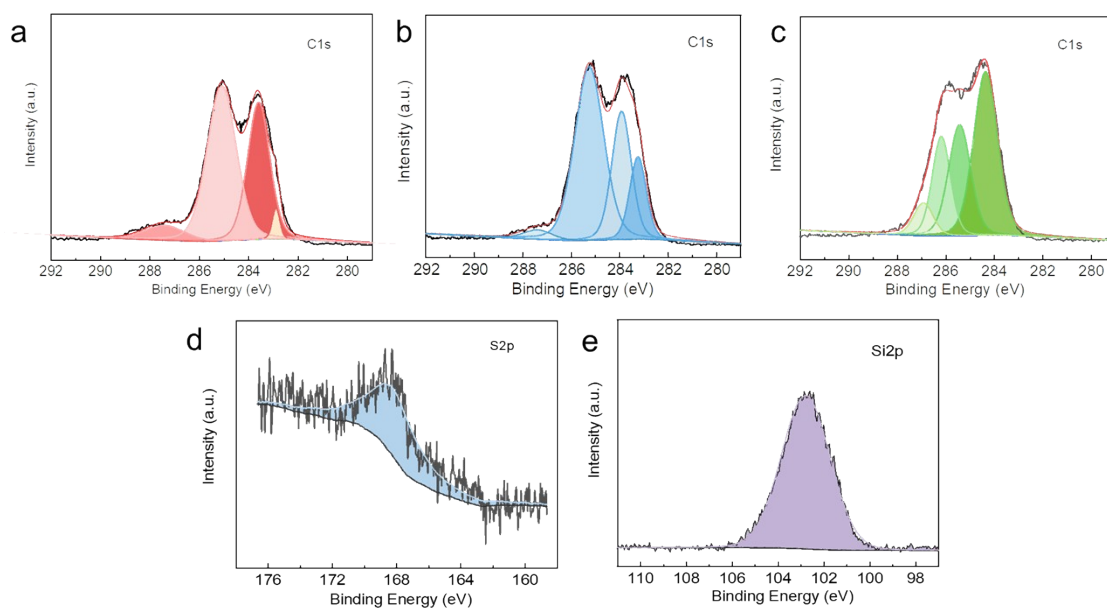size distribution of the (b) PUS sponges and (d) PSiNFs@PU obtained from SEM.

3

Figure S4. High resolution XPS spectra of C1s of (a) PUS, (b) PDA@PU, and (c) PSiNFs@PU. High resolution XPS spectra of (d) S2p and (e) Si2p of PSiNFs@PU. All the above tests were conducted at an environmental temperature of 25 °C.
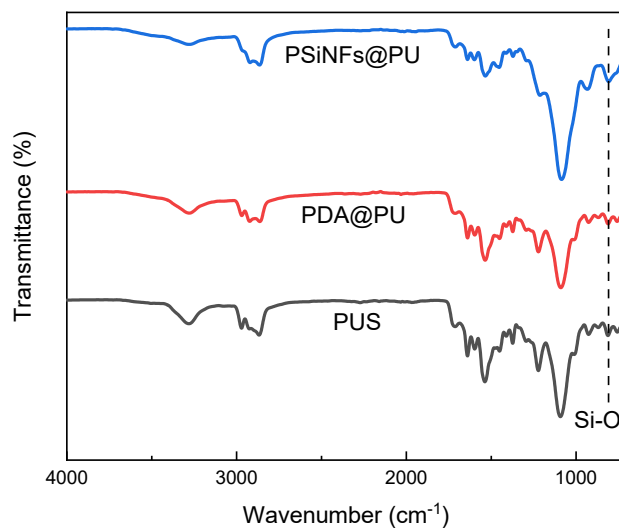

Figure S5. FTIR curves of PUS, PDA@PU, and PSiNFs@PU, respectively. All the above tests were conducted at an environmental temperature of 25 °C.
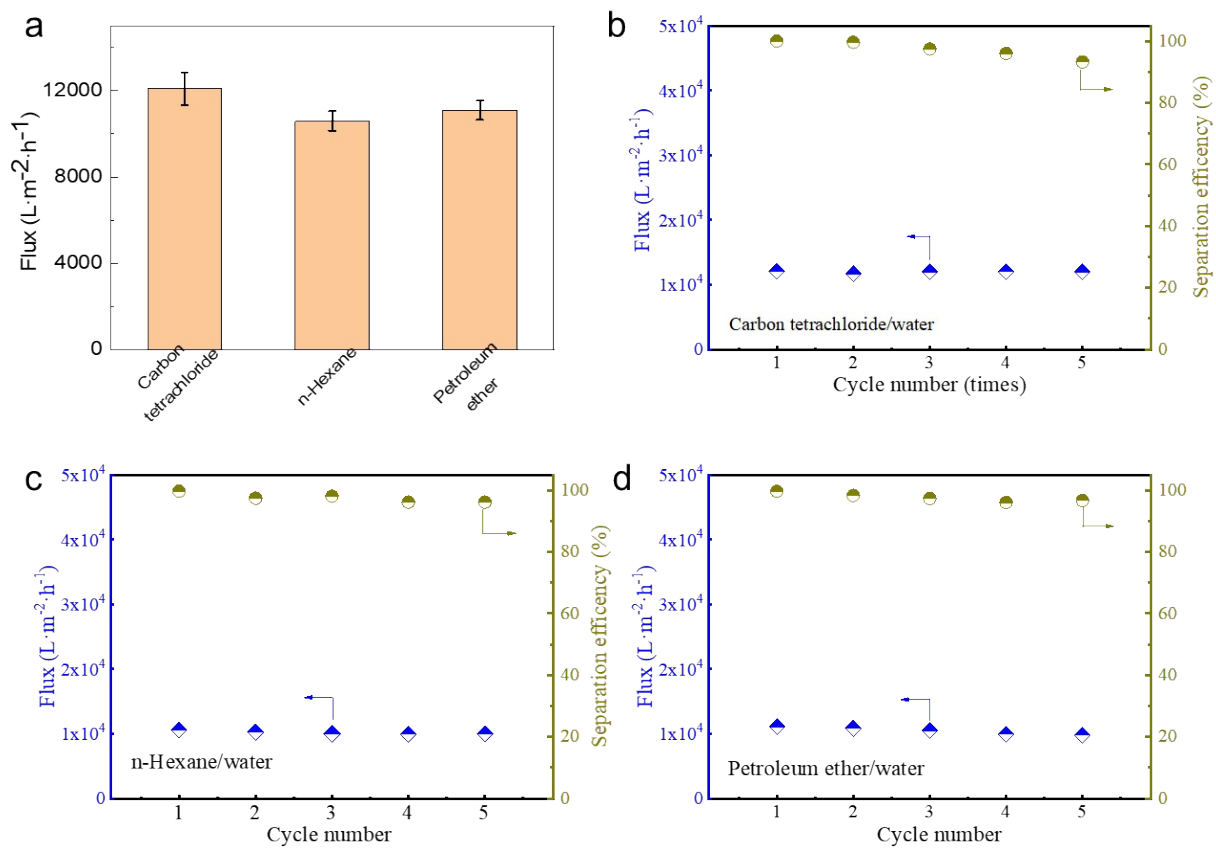
Figure S6. Separation performance of the PSiNFs@PU sponges. (a) Surfactant-stabilized water in oil emulsions separation. Cycling performance of the PSiNFs@PU sponges: (b) carbon tetrachloride/water emulsion, (c) n-hexane/water emulsion, and (d) petroleum ether/water emulsion.
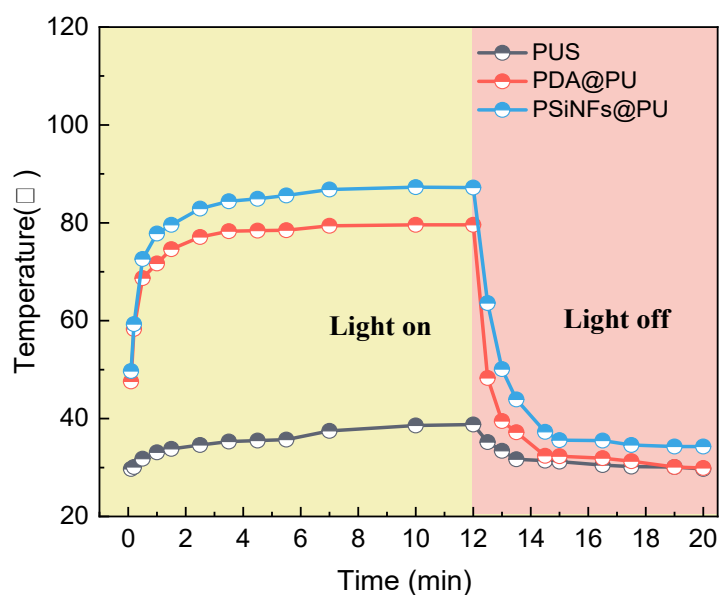
Figure S7. Time-dependent temperature evolution curves of different sponges under one sun illumination (power density: 1.00 kW /m², the yellow and pink region represent temperature-rise and temperature-fall period). All the above tests were conducted at an environmental temperature of 25 °C.
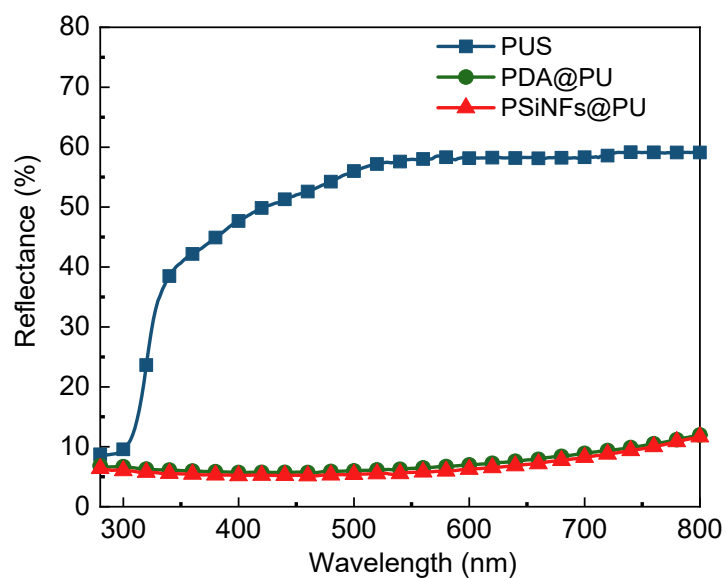

Figure S8. Reflectance spectra of the PUS, PDA@PU, and PSiNFs@PU. All the above tests were conducted at an environmental temperature of 25 °C.
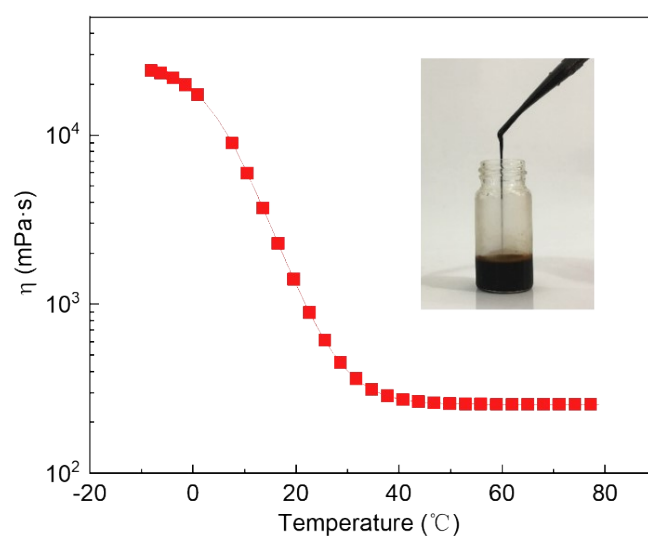
Figure S9. Viscosity changes of crude oil as a function of oil temperature (the shear rate is 1 s^{-1}). The inset image is the crude oils at 0 °C. The test was conducted at an environmental temperature of 25 °C.
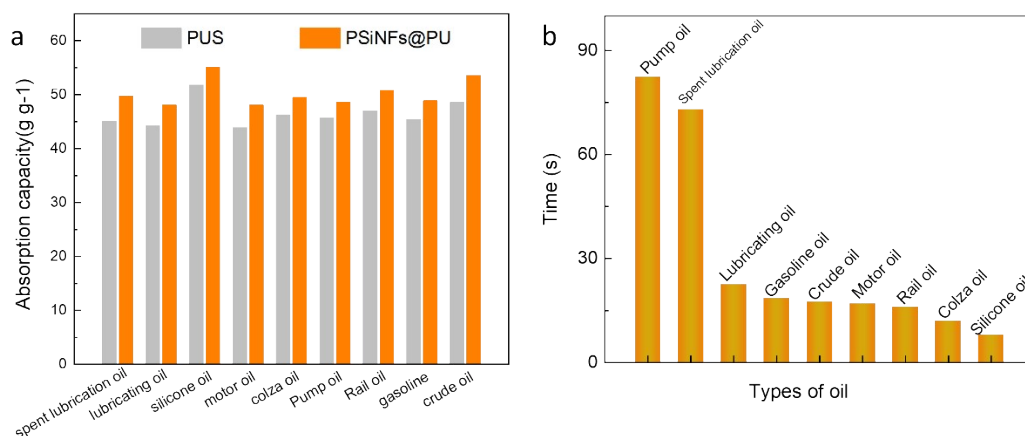

Figure S10. (a) Mass-based absorption capacity of the PUS and PSiNFs@PU sponges for various oils (power density: 1.00 kW /m^2). (b) The time required for the PSiNFs@PU sponges to absorb all types of oil to saturated state (power density: 1.00 kW /m^2). All the above tests were conducted at an environmental temperature of 25 °C.
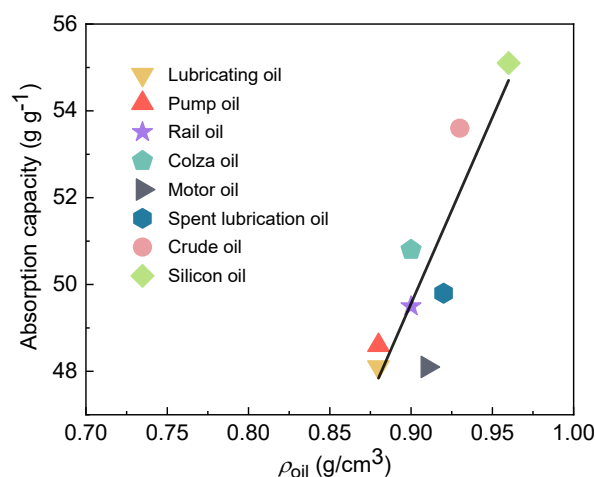
Figure S11. The relationship between the saturation capacity of oil absorption and the density of oil of the PSiNFs@PU sponges (the solid line is the fitted curve). All the above tests were conducted at an environmental temperature of 25 °C.
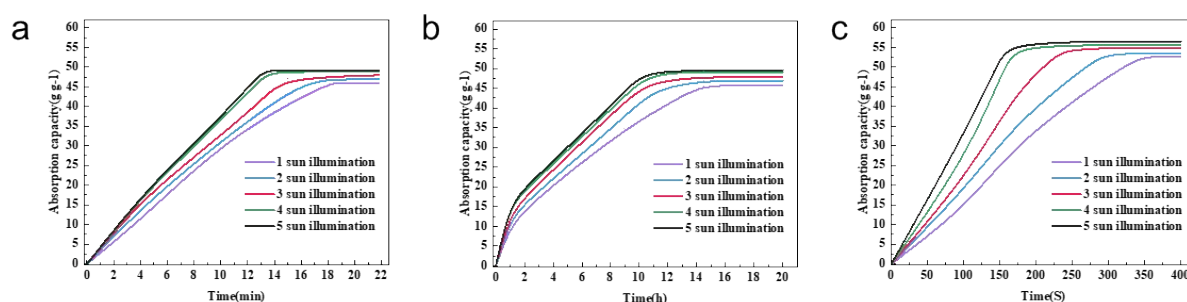

Figure S12. The oil absorption capacity versus time for the PUS (a), PDA@PU (b), and PSiNFs@PU (c), respectively. All the above tests were conducted at an environmental temperature of 25 °C.

Table S1 Adsorption capacity of different absorbents reported in the literature

Material	Absorbed organics	Capacity[k]	
Fe$_3$O$_4$/HDPE PU sponge	Toluene, hexane, dichloromethane, chloroform, cook oil, carbon tetrachloride	15-52	1
Fe$_3$O$_4$-TMHFDS, TEOS/PU sponge	Peanut oil, pump oil, and silicone oil	39-46	2
Fe$_3$O$_4$@GO@OTS PU sponge	Lubricating oil, peanut oil, hexadecane, octane, hexane, heptane	9-27	3
F-MoS$_2$-PU sponge	Hexane, diethyl ether, ethanol, toluene, rapeseed oil, acetonitrile, dichloromethane and chloroform	25-90	4
NDs-PDA-PFDT-PU sponge	Chloroform, diesel, pump oil, gasoline, ethanol, toluene, hexadecane, hexane	4-60	5
CNT/PDMS-PU sponge	Soybean oil, used motor oil, diesel oil, n-hexadecane, gasoline, n-hexane	15-25	6
Polymer molecular brush/PU sponge	Crude oil, Peanut oil, Toluene, Acetone Chloroform, n-hexane Petroleum ether	17-40	7
Fe$_3$O$_4$-graphene PU sponge	lubricating oil, paraffin oil, hydraulic oil, peanut oil, n-hexadecane, heptane	9-27	3
PDA-ZIF-8 melamine sponge	Petroleum ether, Chloroform, Tetrahydrofuran, Gasoline, Toluene, Dodecane	10–38	8
PSiNFs@PU	Crude oil, gasoline, lubricating oil, Pumping oil, Colza oil, Rail oil, motor oil	45-55	**Present work**

[k] Refers to the times of the weight of adsorbed substances *vs.* the weight of adsorbent.
HDPE: high-density polyethylene, TMHFDS: trimethoxy (1H, 1H, 2H, 2H-heptadecafluorodecyl) silane, TEOS: tetraethoxysilane, GO: graphene oxide, OTS: octadecyltrichlorosilane, PU: polyurethane, NDs: nanodiamonds, PDA: polydopamine, PFDT: 1H,1H,2H,2H-perflfluorodecanethiol, CNT: carbon nanotubes, PDMS: polydimethylsiloxane.
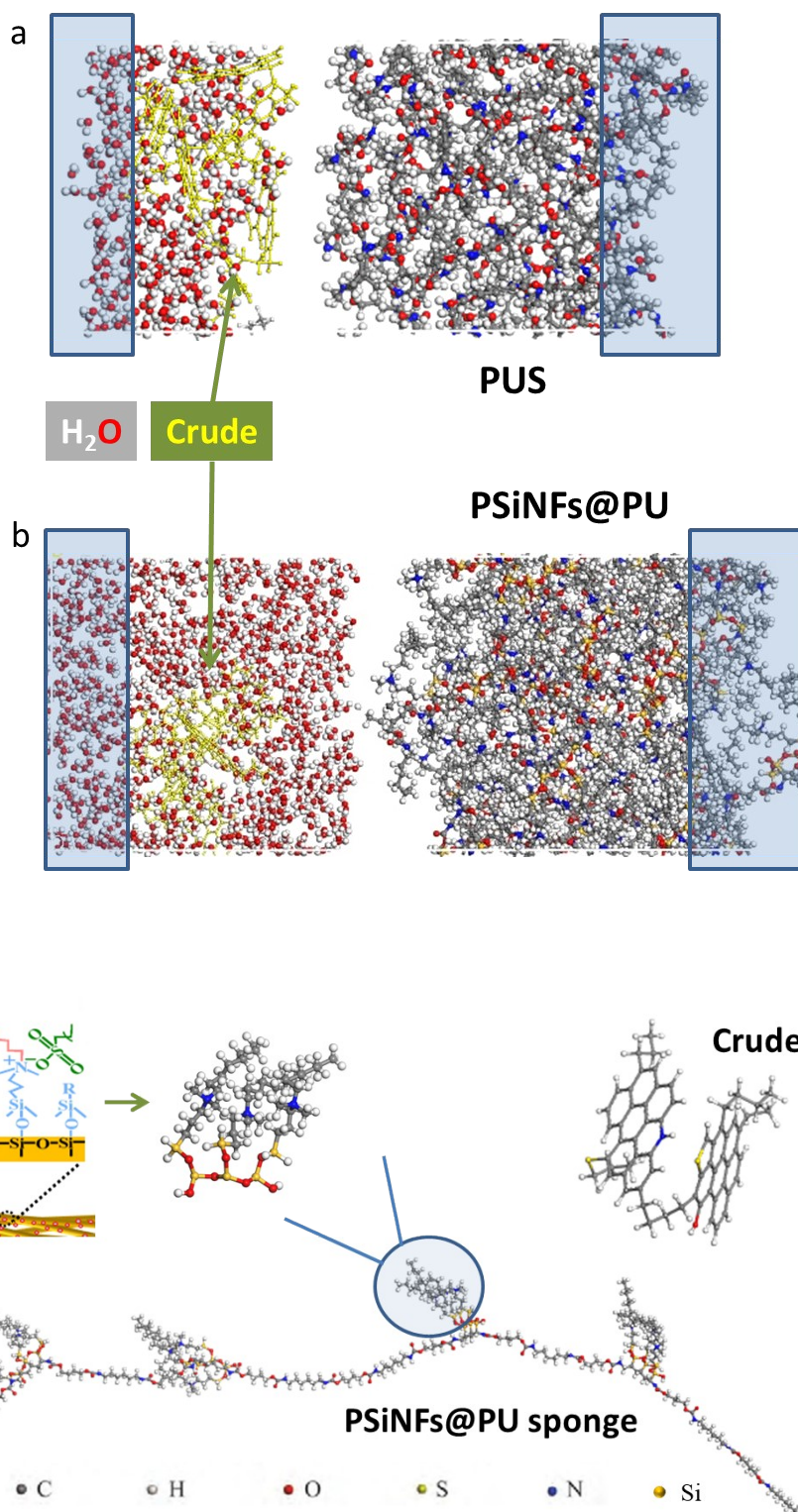
Figure S13. Interface model of crude oil diffusion from water to (a) PUS and (b) PSiNFs@PU.
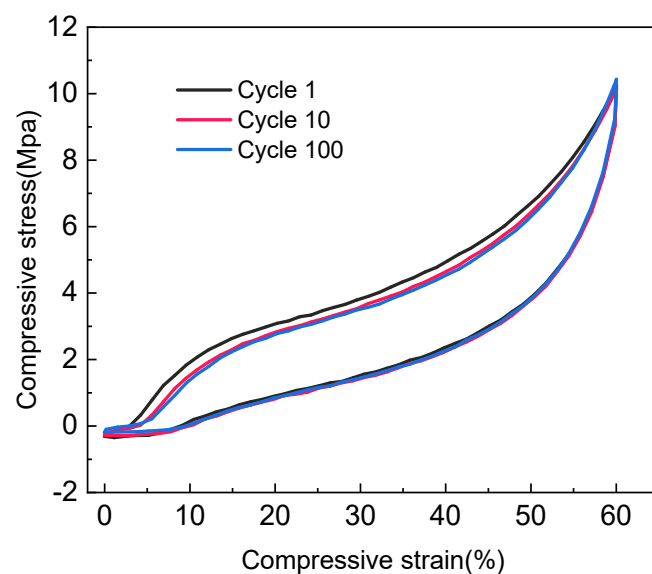
Figure S14. Strain–stress curves of the PSiNFs@PU sponges with cyclic compression under 60% compressive strains. The tests were conducted at an environmental temperature of 25 °C.

Figure S15. Compression recovery of the PSiNFs@PU sponge at 60 % compression strain. The tests were conducted at an environmental temperature of 25 °C.
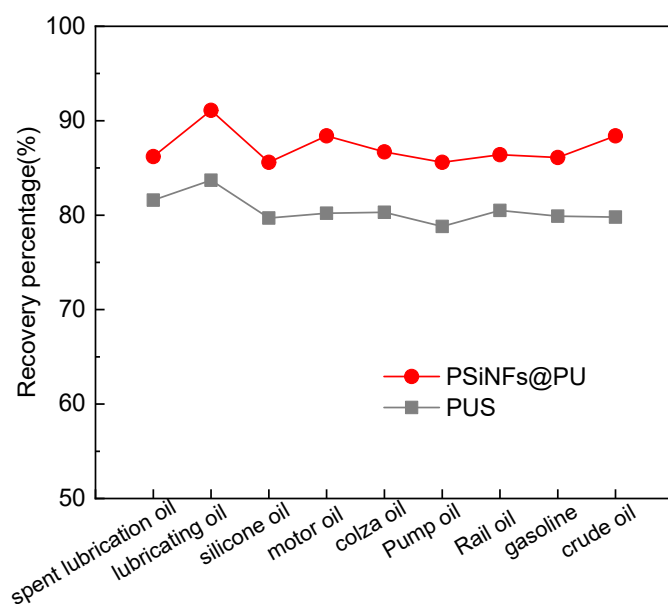
Figure S16. Mass-based squeeze capacity of the PSiNFs@PU sponges for various oils without sun condition. The tests were conducted at an environmental temperature of 25 °C.
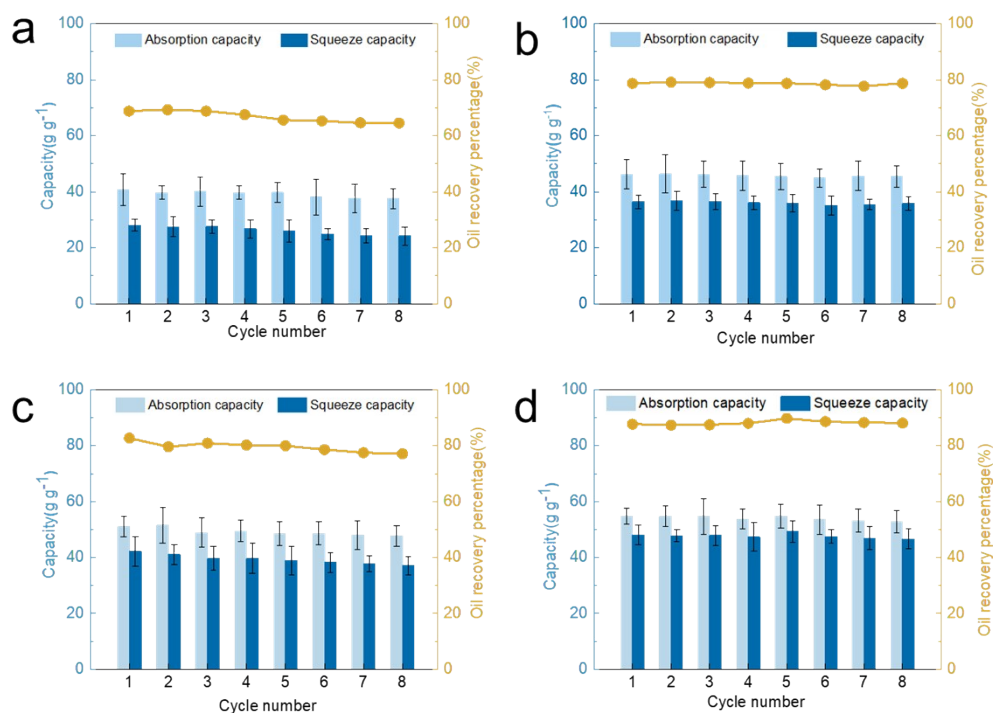

Figure S17. The amount of oil absorbed, squeezed and the recovery rate of the PUS (a) and PSiNFs@PU (b) at no sun illumination. The amount of oil absorbed, squeezed and the recovery

rate of the PUS (c) and PSiNFs@PU (d) at one sun illumination. The tests were conducted at an environmental temperature of 25 °C.
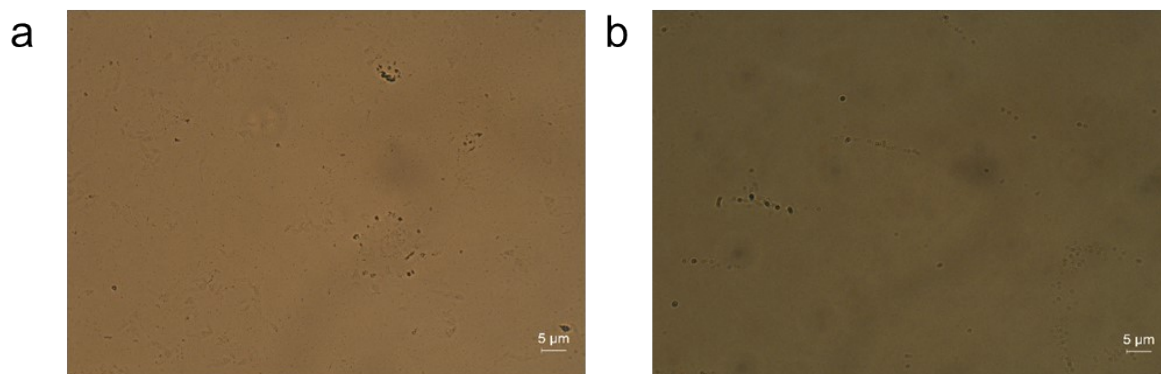

Figure S18. POM images of (a) orignal crude oil and (b) recovery crude oil extruded from the PSiNFs@PU sponges. The tests were conducted at an environmental temperature of 25 °C.
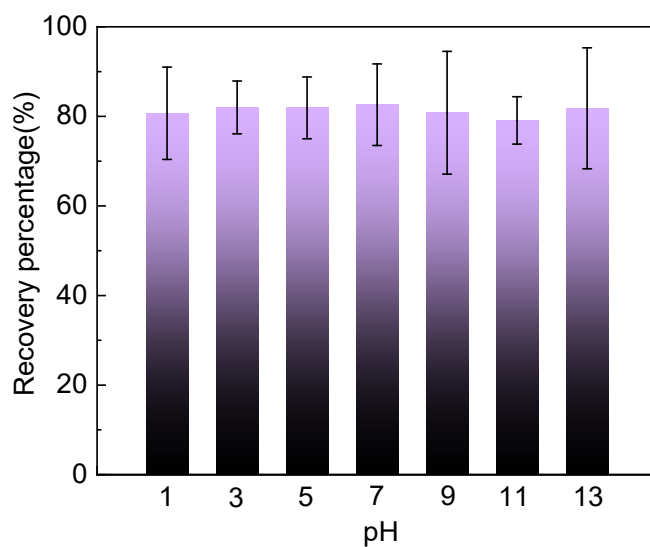

Figure S19. Crude oil recovery performance of the PSiNFs@PU at different pH values without sun illumination. The tests were conducted at an environmental temperature of 25 °C.

Figure S20. Photograph of continuous oil absorption of the PSiNFs@PU sponge under light condition (power density: 1.00 kW /m^2). The tests were conducted at an environmental temperature of 25 °C.

Reference

1.   T. Yu, F. Halouane, D. Mathias, A. Barras, Z. Wang, A. Lv, S. Lu, W. Xu, D. Meziane, N. Tiercelin, S. Szunerits and R. Boukherroub, *Chemical Engineering Journal*, 2020, **384**.
2.   Z.-T. Li, B. Lin, L.-W. Jiang, E.-C. Lin, J. Chen, S.-J. Zhang, Y.-W. Tang, F.-A. He and D.-H. Li, *Applied Surface Science*, 2018, **427**, 56-64.
3.   C. Liu, J. Yang, Y. Tang, L. Yin, H. Tang and C. Li, *Colloids and Surfaces A: Physicochemical and Engineering Aspects*, 2015, **468**, 10-16.
4.   T. Yu, D. Mathias, S. Lu, W. Xu, M. Naushad, S. Szunerits and R. Boukherroub, *Separation and Purification Technology*, 2020, **238**.
5.   N. Cao, B. Yang, A. Barras, S. Szunerits and R. Boukherroub, *Chemical Engineering Journal*, 2017, **307**, 319-325.
6.   C. F. Wang and S. J. Lin, *ACS applied materials & interfaces*, 2013, **5**, 8861-8864.
7.   G. Wang, Z. Zeng, X. Wu, T. Ren, J. Han and Q. Xue, *Polymer Chemistry*, 2014, **5**, 5942-5948.
8.   Z. Lei, Y. Deng and C. Wang, *Journal of Materials Chemistry A*, 2018, **6**, 3258-3263.